Int. Journal of Refractory Metals and Hard Materials 29 (2011) 333–340

Contents lists available at ScienceDirect

Int. Journal of Refractory Metals and Hard Materials

journal homepage: www.elsevier.com/locate/IJRMHM

Compressive strength, hardness and fracture toughness of Al_2O_3 whiskers reinforced ZTA and ATZ nanocomposites: Weibull analysis

A. Nevarez-Rascon [a,1], A. Aguilar-Elguezabal [b], E. Orrantia [b], M.H. Bocanegra-Bernal [b,*]

[a] Escuela de Odontologia, Universidad Autonoma de Chihuahua, Chihuahua, Mexico
[b] Centro de Investigación en Materiales Avanzados, CIMAV S.C., Laboratorio Nacional de Nanotecnologia, Miguel de Cervantes # 120, Chihuahua, Chihuahua, Mexico

ARTICLE INFO

Article history:
Received 28 June 2010
Accepted 15 December 2010

Keywords:
Zirconia
Alumina
Whisker
Characteristic strength
Fracture toughness
Weibull modulus

ABSTRACT

The aim of this investigation was to study the variability in compressive strength, fracture toughness and microhardness applying the well-known Weibull statistics and to be able to provide a wide spectrum of mechanical properties in Al_2O_3 whisker reinforced alumina toughened zirconia (ATZ) and zirconia toughened alumina (ZTA) nanocomposites for possible dental applications. Uniaxial compression tests at room temperature of samples 6.35 ± 0.03 mm in diameter and 12.50 ± 0.63 mm in length and Vickers hardness measurements on polished surfaces were carried out. The indentation fracture toughness (K_{IC}) was derived from the average crack length. Weibull analysis was performed on the data. The ATZ2 (18.0 wt.% Al_2O_3 + 2.0 wt.%$_{(w)}$ + 80.0 wt.% ZrO_2 (TZ-3Y)) nanocomposite reported the highest average compressive load of 1200 MPa, the highest value of characteristic strength, σ_o, of 1340 MPa with Weibull modulus of 3.25 and relatively high fracture toughness (4.7 ± 0.7 MPa $m^{1/2}$), suggesting that with the wide range of mechanical properties obtained in our work, different dental applications could be offered without lead to premature failure.

1. Introduction

The development of new technologies for the manufacture of new dental ceramic materials becomes more important in dentistry in the last decades [1–3] and has been motivated by the demand of materials capable to support new specifications and applications [4] due to their improved esthetics and biocompatibility in comparison with the traditional metal–ceramic restorations [5,6]. All-ceramic restorations such as crowns and bridges, are available on the market and most of them are manufactured with ceramic materials of the types feldspathic ceramic, glass ceramic, and glass-infiltrated ceramic [7,8]. Recently, alumina and zirconia or combination of them [4,5,7,9] has been added to this list. An important lot of research work has been done focusing on the improvement of properties using a combination of Al_2O_3 and ZrO_2 [10,11].

The demand of structural ceramics has led to an increased interest in the processing and characterization of fiber reinforced ceramic composite systems [12]. There are extensive studies on the incorporation of strong ceramic whiskers into ceramic matrices to form a whisker reinforced ceramic matrix composite [13–15] in order to increase the fracture resistance. Xu et al. [16] found that ceramic whisker reinforcement imparted a nearly two-fold increase in the flexural strength and fracture toughness of dental resin composites. On the other hand, the addition of dispersed ZrO_2 should allow an increase in toughness by the initiation of the martensitic transformation of tetragonal ZrO_2 and/or microcracking [17–19].

In the ZrO_2–Al_2O_3 system, two composite materials can be prepared as follows: ZrO_2 reinforced with alumina particles and denominated as ATZ, or Al_2O_3 reinforced with zirconia particles, ZTA. With both composites higher fracture values can be reached when compared with the monophase ceramics [20–22]. To improve the in-service reliability, the introduction of these systems to the dental restorative armamentarium could increase the reliability of all-ceramic crown and bridge restorations as consequence of the transformation toughening mechanism [23–26] which increases its crack propagation resistance. Nevertheless, it is well known that dental restorative ceramics and composites are susceptible to brittle fracture and no standard method exist to predict this type of failure [27] due to its complex geometry [3]. Ceramic materials generally fail by the unstable extension of flaws [28] which could involve pores, inclusions, distributed microcracks, or many other possible variations and combinations [27] producing a considerable variability in their mechanical properties [29]. In this context, the reliability of brittle ceramics under loading has to be described by a probabilistic function (statistics) [30].

Years ago, Weibull [31,32] proposed a statistical theory of brittle fracture that up to these days is the basis of the state of the art in mechanical design procedure of ceramic components [30]. Considering physical assumptions, the multiaxial Weibull theory describes the effect of a multiaxial stress distribution in a component on the

* Corresponding author. Tel.: +52 614 4394801; fax: +52 614 4394823.
E-mail address: miguel.bocanegra@cimav.edu.mx (M.H. Bocanegra-Bernal).
[1] Now with Escuela de Odontología, Universidad Juárez del Estado de Durango, Durango, México.

0263-4368/$ – see front matter © 2010 Elsevier Ltd. All rights reserved.
doi:10.1016/j.ijrmhm.2010.12.008

strength [28] distribution where the failure probability (P_f) is given by the following relation:

$$P_f = 1\text{–}\exp\left[-\left(\frac{\sigma}{\sigma_0}\right)^m\right], \quad (1)$$

where σ_o is the scale parameter and m is the shape parameter or alternatively referred to as the Weibull modulus and is found by linear regression (widely used due to its simplicity) on a plot of ln ln $[1/(1-P_f)]$ against ln (fracture stress). The slope of the line is therefore, the Weibull modulus and has a value between 5 and 20 for technical ceramics [33,34] and some ceramic materials fabricated in a dental laboratory [35–37]. On the other hand, the scale parameter or characteristic strength, σ_o, is the value of stress for which ln ln $[1/(1-P_f)]$ is zero, or $P_f = 63.2\%$ [27,32,33]. For determining the probability of failure P_f an estimator must be used [38] for each data point. Two different estimators have been widely used according to the following expressions [39,40]

$$P_f = \frac{i}{(N+1)} \quad (2)$$

and

$$P_f = \frac{(i-0.5)}{N}, \quad (3)$$

where i is the ranking of the strength and N the total of experimented samples. How to prepare a Weibull strength distribution graph is clearly presented in Ref. [27]. It has been shown that the Eq. (2) corresponds to the median probability of failure and Monte Carlo simulation technique [41], has shown that the more conservative m and reliability predictions using this modulus gives the least bias and from engineering and materials science point of view is therefore preferred [34,38].

Considering that the Weibull distribution has been widely used to characterize mechanical testing data, several investigations have been carried out on different materials. For example Green and Campbell [42] showed that the tensile strength of cast Al–Si alloys follow a Weibull distribution, Guazzato et al. [23] investigated on glass-infiltrated Al_2O_3–ZrO_2 composite (Inceram–Zirconia) and obtained considerably lower strength ($\sigma_o = 582$ MPa with Weibull modulus $m = 8.9$) in comparison to the zirconia specimens, Bona et al. [37] reported values of Weibull modulus, m, between 5 and 14 for different commercial hot-pressed (HP) dental ceramics, and Gong et al. [43] studied the variability of the measured indentation toughness modeled by the well-known Weibull statistics. To the knowledge of the authors and considering a lack of information concerning the Weibull analysis of compressive strength and fracture toughness of Al_2O_3 whisker reinforced ATZ and ZTA nanocomposites for possible dental applications, the aim of this investigation was to offer a wide spectrum of mechanical properties which could fulfill the requirements for applications in posterior frameworks where mastication forces ranging from 50 to 250 MPa in normal mastication, and 500–880 MPa in parafunctional behavior such as bruxism [7,44,45]. With this background, we believe that our results with ATZ and ZTA nanocomposites could offer great possibilities for the manufacture of dental restorations such as frameworks for four-unit posterior fixed partial dentures (FPDs) reducing the prolonged times required for computer-aided design (CAD)/computer-aided manufacturing (CAM) without sacrificing the minimum hardness and fracture toughness required for these applications.

2. Materials and methods

2.1. Mixture preparation

High purity α-Al_2O_3 (Baikalox SM8, Baikowski, USA; 100% α, purity>99.99%), MgO (500A, UBE Chemical Industries, Japan; purity>99.999%), and ZrO_2 + 3 mol% Y_2O_3 (thereafter abridged as TZ-3Y, Tosoh, Japan; purity>99.99%) powders and Al_2O_3 whiskers (2–4 nm × 2800 nm, Aldrich, USA) were used as starting materials. Table 1 summarizes their characteristics (particle size, surface area and theoretical density). Homogeneous mixtures of Al_2O_3 + 20 wt.% TZ-3Y + Al_2O_{3w} (0.5, 1, 1.5, and 2 wt.%) for the ZTA system, and TZ-3Y + 20 wt.% Al_2O_3 + Al_2O_{3w} (0.5, 1, 1.5, and 2 wt.%) for the system ATZ were prepared. Pure TZ-3Y and Al_2O_3 as well as ZTA and ATZ composites without addition of alumina whiskers, were also prepared for comparison. For convenience, the compositions were identified as follows: i) the pure monolithic Al_2O_3 and TZ-3Y specimens are referred to as A, and Z, respectively; ii) pure ATZ and pure ZTA samples are referred to as ATZ, and ZTA, respectively; iii) ATZ with additions of 0.5, 1, 1.5, and 2 wt.% Al_2O_3 whiskers are referred to as ATZ0.5, ATZ1, ATZ1.5, and ATZ2, respectively, and iv) ZTA with additions of 0.5, 1, 1.5, and 2 wt.% Al_2O_3 whiskers are referred to as ZTA0.5, ZTA1, ZTA1.5, and ZTA2, respectively. The identification codes for each composition are summarized in Table 2. Whiskers were firstly dispersed in 200 mL ethanol by ultrasonic vibration for 45 min to destroy the agglomeration state. Then, the nanopowders were magnetically stirred along with the dispersed Al_2O_3 whiskers for 3 h at 40 °C until most of the ethanol evaporated and then the resulting powder mixtures were dried at 100 °C for 12 h. In all compositions, the Al_2O_3 powder was previously doped with 25 ppm of MgO powder in order to inhibit the grain growth during sintering.

Table 1
Characteristics of commercial starting powders.

Powder	Primary particle size (μm)	BET surface area ($m^2\ g^{-1}$)	Theoretical density ($g\ cm^{-3}$)
Baikalox SM8 Al_2O_3[a]	0.050	10.0	3.98
3 mol% Y_2O_3–ZrO_2 (TZ-3Y TOSOH)[b]	0.075	17.2	6.05
MgO 500A[c]	0.053	31.9	3.58
Al_2O_3 whiskers Ø 2–4 nm, length 2800 nm[d]		125	4.00

[a] Supplied by Baikowski (USA).
[b] Supplied by TOSOH (Japan).
[c] Supplied by UBE Chemical Industries (Japan).
[d] Supplied by Sigma Aldrich (USA).

2.2. Compaction and sintering

The mixtures were uniaxially pressed at 50 MPa in a steel mold (16 mm in diameter size) using an Elvec Hydraulic Press (by ELVEC S. A. de C.V., Mexico) at a constant strain rate. Green Samples were placed into an alumina crucible with ZrO_2 + Al_2O_3 bed powders and sintered at 1500 °C for 2 h in air at a heating rate of 10 °C min^{-1}. After sintering, the furnace was shut off and it was allowed to cool down. Densities were measured with a Multipycnometer (by Quantachrome Instruments, USA) using Helium as displacement gas for the as-

Table 2
Compositions and identification codes.

Composition	Identification
Pure Al_2O_3	A
80.0 wt.% Al_2O_3 + 20 wt.% TZ-3Y	ZTA
79.5 wt.%Al_2O_3 + 0.5 wt.%$_{(w)}$ + 20 wt.% TZ-3Y	ZTA0.5
79.0 wt.% Al_2O_3 + 1.0 wt.%$_{(w)}$ + 20 wt.% TZ-3Y	ZTA1
78.5 wt.% Al_2O_3 + 1.5 wt.%$_{(w)}$ + 20 wt.% TZ-3Y	ZTA1.5
78.0 wt.% Al_2O_3 + 2.0 wt.%$_{(w)}$ + 20 wt.% TZ-3Y	ZTA2
20.0 wt.% Al_2O_3 + 80 wt.% TZ-3Y	ATZ
19.5 wt.% Al_2O_3 + 0.5 wt.%$_{(w)}$ + 80% TZ-3Y	ATZ0.5
19.0 wt.% Al_2O_3 + 1.0 wt.%$_{(w)}$ + 80% TZ-3Y	ATZ1
18.5 wt.% Al_2O_3 + 1.5 wt.%$_{(w)}$ + 80% TZ-3Y	ATZ1.5
18.0 wt.% Al_2O_3 + 2.0 wt.%$_{(w)}$ + 80% TZ-3Y	ATZ2
Pure TZ-3Y	Z

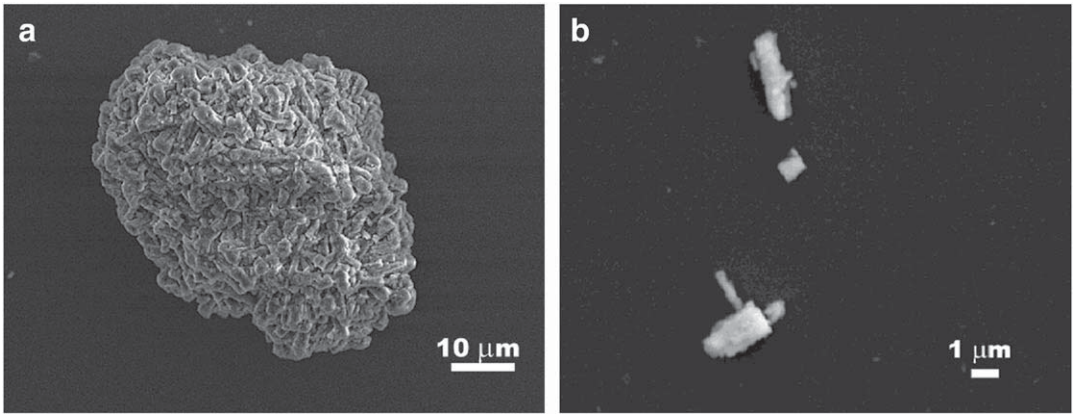

Fig. 1. SEM micrographs showing the appearance of the Al_2O_3 whiskers. (a) Agglomerate of "as received" whiskers and (b) higher magnification of whiskers after dispersing them in ethanol.

sintered samples at least 3 times and the measured values were averaged. The samples were ground and polished through SiC paper in sequence of # 600, # 800, # 1000 and # 1200, and then polished by diamond pastes of both 0.5 and 0.25 μm and subsequently thermally etched in air for 40–60 min at the temperature of 150 °C below the sintering temperature.

2.3. Samples characterization

The polished and fracture surfaces as well as the Al_2O_3 whiskers (a very small amount of them were dispersed on a cooper sheet) were characterized by Scanning Electron Microscopy (SEM: JEOL JSM 5800 LV, Japan, and FEG SEM: JEOL JMS 7000 F, Tokyo, Japan) using an accelerating voltage of 2–10 kV. The average grain size of ATZ and ZTA composites was measured by standard linear intercept technique and at least 400–500 grains in each sample were measured.

2.4. Compressive strength, hardness and fracture toughness

Uniaxial compression testing was conducted at room temperature using an Elvec Hydraulic Press (by ELVEC S.A. de C.V., Mexico) applying a load rate of 45 kN min^{-1}.The test specimens for Weibull analysis were 6.35 ± 0.03 in diameter and 12.50 ± 0.63 mm in length following the standard ASTM C 1424-99 [46]. The loading surfaces were polished to be parallel to an accuracy of less than 15 μm. Vickers hardness measurements were carried out on sintered samples by using a Microhardness Tester FM-7 (by Future-Tech, Tokyo, Japan). Three samples per composition (with diameter of 12 mm, and thickness of 5 mm) and approximately 20–30 indents per measurement were made and the average hardness was determined. The separation between neighboring indentations was more than four diagonal lengths of indentation impression according to the standard ASTM C 1327-99 for Vickers indentation hardness of advanced ceramics [47]. The corresponding indentation sizes and crack lengths were measured using an optical microscope Olympus PMG3 (by Olympus Co., Japan). In the present work the cracks appeared on polished surfaces for a load of 1 kg held for 15 s. The indentation fracture toughness (K_{IC}) was derived from the average crack length. For a ratio $c/a > 2.5$ (present study), where c is the crack length and a is the half diagonal length of the indentation impression, K_{IC} is calculated using the following equation [48]:

$$K_{IC} = 0.0752.P/c^{3/2} \quad (4)$$

where K_{IC} is the fracture toughness, P is the load and c is the crack length.

3. Results

SEM micrographs of Al_2O_3 whiskers are shown in Fig. 1. Agglomerates of "as received" whiskers showing a variety of morphologies and sizes exhibiting lengths of several microns with different aspect ratios can be observed in Fig. 1a. Some isolated Al_2O_3 whiskers appear shorter in average after dispersing them in ethanol indicating that they became broken during the processing (Fig. 1b). The variation of relative density (measured density divided by the theoretical density) with the alumina whisker content is shown in Fig. 2. The addition of whiskers up to 1.5 wt.% has no significant influence on the densification behavior though the relative density decreases slightly with the increase of Al_2O_3 whiskers. However, at whiskers content of 2 wt.%, the attainable density decreases significantly in ATZ and ZTA systems. Difficult dispersion of Al_2O_3 whiskers could be the cause for this phenomenon considering some agglomeration state of whiskers as can be seen in Fig. 1a.

The mean values of relative density, grain size, compressive strength, fracture toughness and Vickers hardness are reported in Table 3. It is observed that the compressive strength and fracture toughness values are higher for ATZ composites than ZTA ones. It is very interesting to note that in the ZTA system the compressive strength decreases with increasing of alumina whiskers content. This decrease in compressive strength can be attributed to the large grain size (see Table 3) and to the slight decrease in density as consequence of the agglomeration of Al_2O_3 whiskers that can act as rigid inclusions, impeding sintering mechanisms and causing the inhomogeneity of the phase distributions. The increasing of Al_2O_3 particles on the

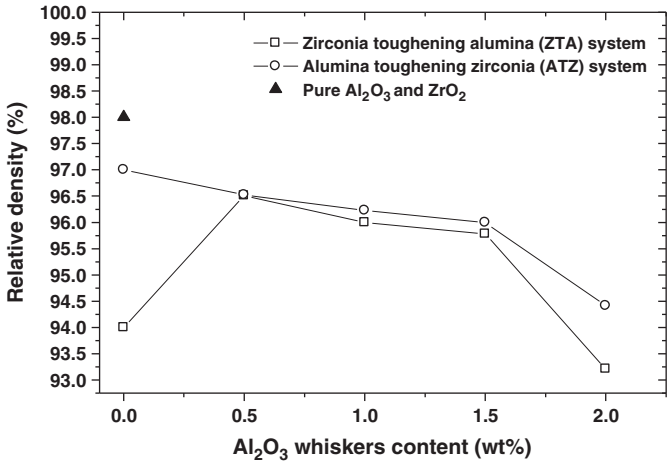

Fig. 2. Relationship between relative density (%) and percentage of Al_2O_3 whiskers content.

Table 3
Relative density, grain size, compressive strength, fracture toughness, and Vickers hardness of different tested composites.

Composition	Relative density (% TD)	Mean grain size (μm) (std.dev.)	Compressive strength (MPa) (std. dev.)	Fracture toughness (MPa $m^{1/2}$) (std. dev.)	Vickers hardness (GPa) (std. dev.)
A	98.00	1.27 (0.60)	618.6 (436.6)	4.2 (0.4)	21.9 (1.7)
ZTA	94.00	0.59 (0.10)	484.3 (308.2)	5.1 (1.3)	16.1 (3.6)
ZTA0.5	96.51	0.41 (0.21)	603.4 (400.4)	3.0 (0.3)	17.7 (0.9)
ZTA1	96.00	0.42 (0.21)	454.4 (281.2)	3.1 (0.3)	17.2 (1.1)
ZTA1.5	95.78	0.41 (0.20)	420.0 (170.3)	3.7 (0.6)	16.1 (1.6)
ZTA2	93.21	0.40 (0.16)	450.4 (152.0)	3.5 (0.7)	15.2 (2.2)
ATZ	97.00	0.53 (0.12)	879.6 (349.0)	7.4 (0.6)	14.0 (1.3)
ATZ0.5	96.52	0.39 (0.16)	749.0 (360.6)	4.7 (0.4)	13.3 (0.9)
ATZ1	96.23	0.37 (0.15)	869.2 (436.7)	4.4 (0.7)	12.7 (0.8)
ATZ1.5	96.00	0.38 (0.17)	904.8 (238.0)	4.6 (0.6)	12.6 (0.8)
ATZ2	94.41	0.37 (0.15)	1199.3 (348.4)	4.7 (0.7)	12.7 (1.1)
Z	98.00	0.57 (0.12)	522.2 (185.5)	6.4 (0.4)	13.7 (0.5)

composition of ZTA composites leads to the grain size increasing in both phases, ZrO_2 and Al_2O_3. An inverse phenomenon is observed with the ATZ system where the sintered densities slightly increased and the grain size diminished (see Table 3). On the other hand, a slight increase in fracture toughness with the alumina whiskers content is observed in ZTA composites while this value is practically constant for the ATZ composites. Taking into account that the ATZ2 sample reported the higher value of compressive strength and relatively high fracture toughness, we will make reference thereafter to the ATZ2 composite and this will be compared with the ZTA2 composite. The relative high fracture toughness (4.7 ± 0.7 MPa $m^{1/2}$) obtained with the composition ATZ2 compared to ZTA2 (3.5 ± 0.7 MPa $m^{1/2}$) can be attributed to the fracture mode. This appreciation can be supported by Fig. 3 where observations at higher magnification of one arm of an indented impression in both ATZ2 and ZTA2 systems, show evidence of crack deflection (zigzagged cracks, arrow marks). In both composites, the fracture pattern is a combination of transgranular and intergranular fractures as can be seen in Fig. 4a–b. Although the Vickers hardness values for ZTA samples were slightly higher than the ATZ ones, the addition of Al_2O_3 whiskers has no significant influence on the measured hardness. However, the slight decreasing in hardness in both systems could be attributed to the sensitivity of hardness to the decrease of the sintered density (Fig. 2). In this context, the obtained hardness values are related to the different remaining porosity in each sample as well as the intrinsic deformability of the ceramic and microstructural parameters such as multiphases, grain size and orientation and boundary constitution [4,15,49,50].

The statistical properties of the compressive strength, fracture toughness and Vickers hardness for the different composites applying Weibull statistics are summarized in Table 4. From this table, it is clear that the Weibull moduli for the compressive strength, Vickers hardness, and fracture toughness measurements in the ATZ2 composite are higher than obtained for ZTA2 composites suggesting that the flaws in ATZ2 ones have rather uniform sizes leading to a relatively high level of structural integrity compared to ZTA2 composites.

4. Discussion

In general, the mechanical failure in ceramic matrix composites occurs when a large number of pre-existing cracks are present which in turn cause a large variability in strength as a consequence of the distribution in crack sizes [37]. An alternate way to improve the

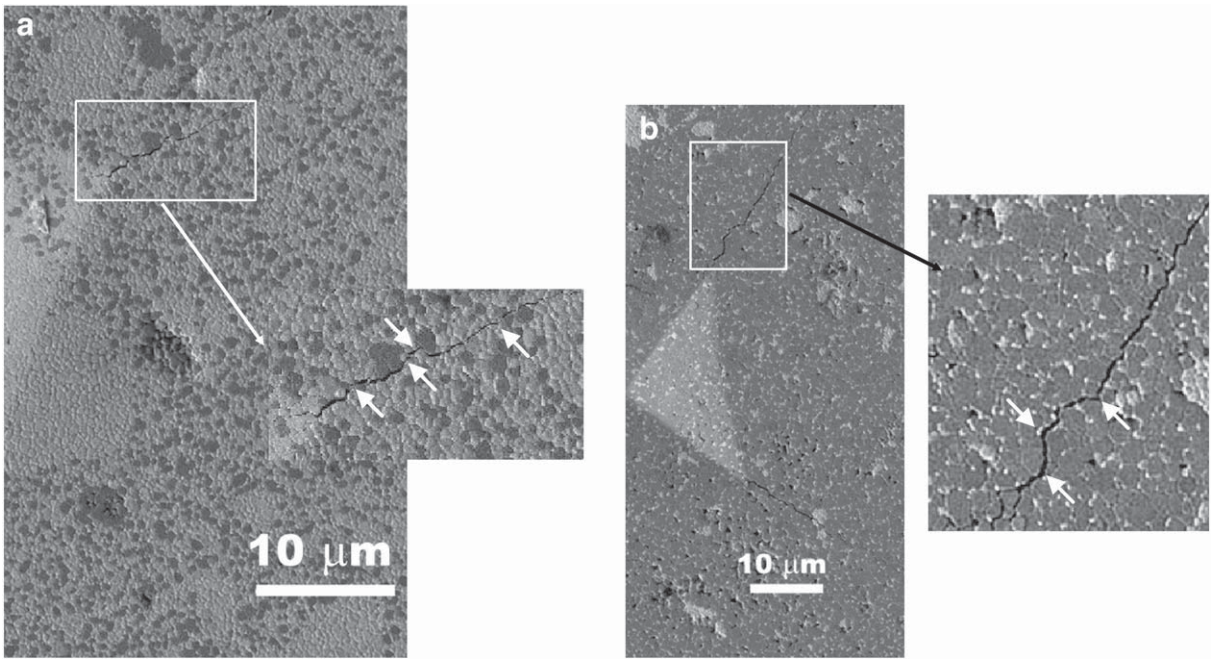

Fig. 3. SEM micrographs of Vickers indentations (a) ATZ2 composite, and ZTA2 composite (b). Arrow marks explained in text.

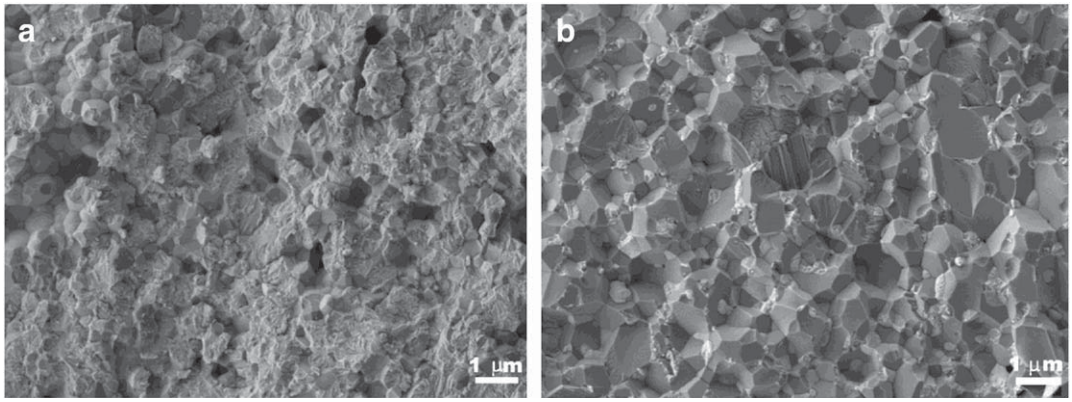

Fig. 4. Representative fracture surfaces of ATZ 2 composite (a), and ZTA2 composite (b).

structural integrity in ATZ and ZTA ceramic composites could be the addition of strong Al_2O_3 whiskers. However, it is very important to obtain whiskers free of agglomerates in order to attain high sintered density. If the whiskers remain in agglomerate state during their processing, these will remain in the final microstructure producing low density regions [51], which is reflected in a low sintered density, as can be observed in Fig. 2 for whiskers content higher than 1.5 wt.% in both ATZ and ZTA systems. The addition of low Al_2O_3 whiskers seems to be enough to increase the hardness in the ZTA system. According to Table 3 the hardness for ATZ system decreases with increasing Al_2O_3 whiskers content. According to Table 3, 2 wt.% whiskers are required to get high fracture toughness in ATZ composites. This behavior can be supported by the results of Chakravarty et al. [52]. Al_2O_3 whiskers ranging from 0.5 to 2.0 wt.%, could be the optimum amount to obtain relatively good mechanical properties considering that with alumina whiskers content higher than 2.0 wt.%, both hardness and fracture toughness values drop dramatically due to aspect ratio and the formation of defects, such as large pores, cluster of whiskers, etc., decreasing the density and mechanical properties of the composite [53]. The deleterious effects of the alumina whisker aspect ratio on the green consolidation as well as sinterability, could act to decrease the beneficial toughening of the whiskers additions resulting in a significant decrease in the fracture toughness of the composite [54].

It is believed that the relative high fracture toughness in the ATZ2 composite could be attributed to the mixed fracture mode (many pits present on the fracture surface) as can be observed in Fig. 4a, where the roughness of the fracture surface increased in comparison to the relatively smooth fracture surface shown in Fig. 4b (ZTA2 composite). A mixed fracture mode could result in greater fracture energy which leads to greater fracture toughness. Likewise, it is noteworthy that the intergranular fracture mode will improve the fracture toughness of the composite by crack deflection (zigzagged cracks) and bridging grains. An increase in toughness may also be due to the high aspect ratio of the Al_2O_3 whiskers as well as a moderate interface bonding which in turn could enhance crack bridging and whisker pull-out mechanism according to Zhang et al. [13] and Becher et al. [55]. In other words, the fracture of the ATZ2 composites is a mixture of transgranular and intergranular modes (Fig. 4a) while the degree of intergranular fracture increases with the increasing Al_2O_3 content (Fig. 4b) resulting in a low fracture toughness as can be seen in Table 3. Therefore, for a constant addition of alumina whiskers, the ATZ composite leads to higher fracture toughness values than the ZTA composite.

On the other hand, the compressive strength in the ATZ composites is higher than the ZTA ones when the Al_2O_3 whiskers content is increased according to what is shown in Table 3. According to standard deviation value for each composition in both ATZ and ZTA composites, a variability in compressive strength (Table 3) can be indicative of the presence of multiple defect distributions [56] such as compositional inhomogeneities, inclusions as well as pores producing an irregular strength. Therefore, the variability of compressive strength, Vickers hardness, and fracture toughness in the ATZ and ZTA composites with additions of 2 wt.% Al_2O_3 whiskers were analyzed using the Weibull statistical method. The Weibull probability plots using Eq. (2) for compressive strength, Vickers hardness, and fracture toughness are given in Fig. 5 (ZTA2 composite) and Fig. 6 (ATZ2 composite). As can be seen, a good linear relationship between $\ln\ln[1/(1-P)]$ and $\ln\sigma$, $\ln H_v$ (Fig. 5a,b) and $\ln\ln[1/(1-P)]$ and $\ln\sigma$, $\ln K_{IC}$ (Fig. 6a,c) was observed indicating that the experimental data can be well described with the Weibull distribution equation. The coefficient of determination (R^2) is considered as a measure of the goodness-of-fit and for $R^2 \geq 0.95$ the fit is good and is associated with a single mode of failure [56] meanwhile for $R^2 < 0.90$, the fit is poor for

Table 4
Statistical properties of the compressive strength, fracture toughness and Vickers hardness measured for different composites.

Composition	Compressive strength				Vickers Hardness			Fracture toughness		
	n	Weibull modulus (m)	R^2	Characteristic strength σ_θ (MPa)	n	Weibull modulus (m)	R^2	n	Weibull modulus (m)	R^2
A	10	1.45	0.91	713	30	18.50	0.97	10	10.09	0.94
ZTA	10	1.49	0.92	573	30	4.72	0.96	10	3.72	0.81
ZTA0.5	10	1.18	0.92	735	30	19.15	0.94	10	9.75	0.98
ZTA1	10	1.83	0.83	528	30	17.78	0.94	10	8.01	0.96
ZTA1.5	10	2.19	0.94	488	30	10.56	0.96	10	5.85	0.96
ZTA2	10	2.75	0.96	513	30	7.14	0.97	10	4.96	0.94
ATZ	10	2.31	0.88	1012	30	11.41	0.98	10	12.22	0.85
ATZ0.5	10	1.87	0.85	880	30	16.16	0.96	10	10.75	0.90
ATZ1	10	1.96	0.90	1012	30	15.78	0.98	10	4.82	0.88
ATZ1.5	10	3.64	0.94	1002	30	16.00	0.98	10	7.00	0.92
ATZ2	10	3.25	0.98	1340	30	12.00	0.92	10	5.85	0.98
Z	10	2.34	0.91	608	30	30.47	0.96	10	17.60	0.94

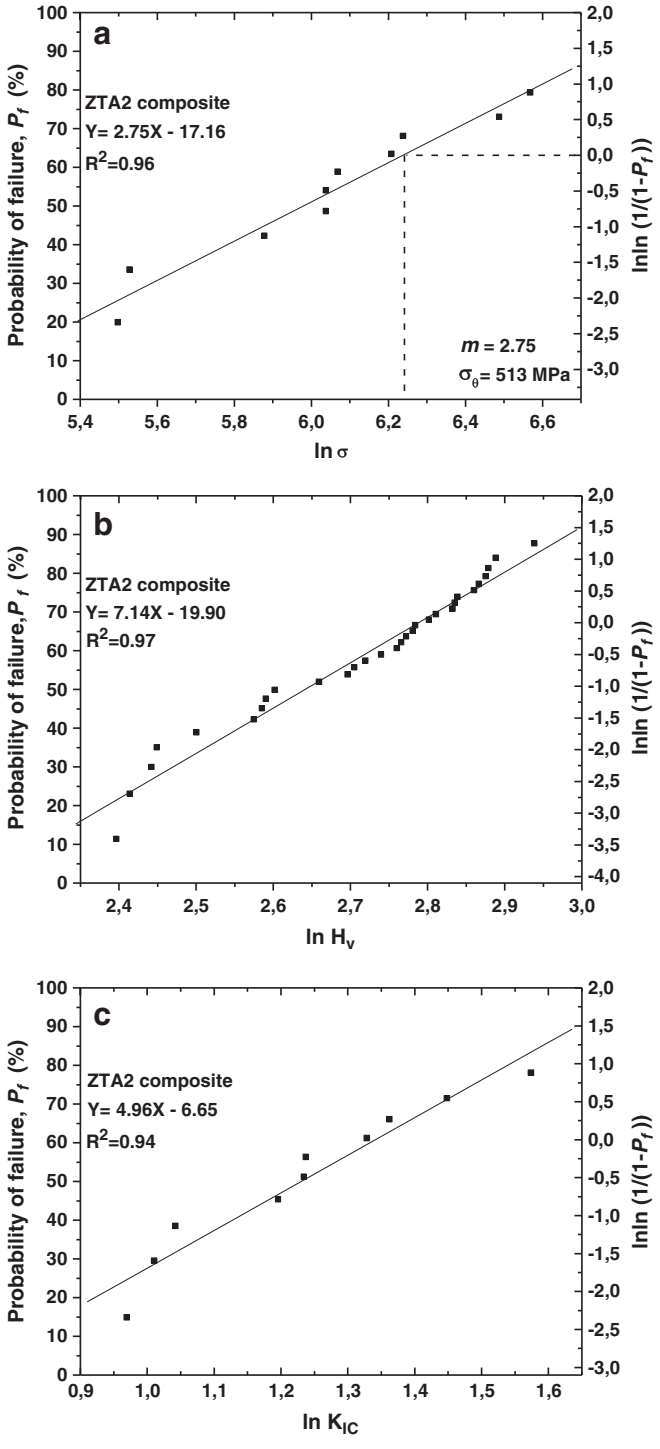

Fig. 5. Weibull plots of the ZTA2 composite. (a) Compressive strength, (b) Vickers hardness, and (c) fracture toughness.

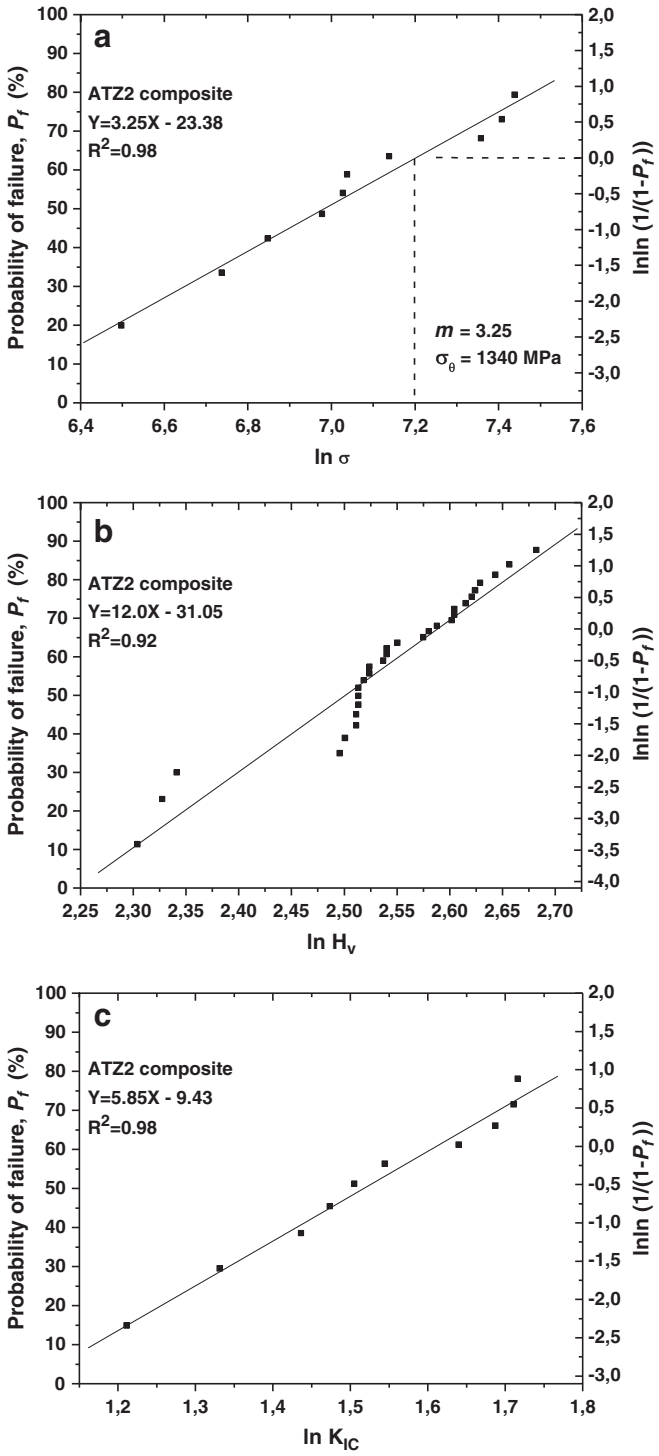

Fig. 6. Weibull graphs for ATZ2 composite. Compressive strength (a), Vickers hardness (b), and fracture toughness (c).

the sample size according to what is stated by Tiryakioglu et al. [57] and Doremus [58]. Likewise, for R^2 between 0.95 and 0.90, no guidance was provided.

The estimated Weibull modulus m (a measure for the scatter of experimental data) and the parameter σ_o (value of stress for which ln ln $[1/(1-P_f)]$ is zero, or $P_f = 63.2\%$) using linear regression method were 2.75 and 513 MPa and 3.25 and 1340 MPa for ZTA2 and ATZ2 composites, respectively (see Table 4, Figs. 5a, and 6a). The increase in Weibull modulus in the ATZ2 ceramics will indicate that the range of flaw sizes decreases with the addition of Al_2O_3 whiskers if these have been properly dispersed in the matrix powders. Conversely, the flaws size/distribution would increase with increasing Al_2O_3 whisker content. Likewise, it is believed that an increase of compressive strength in the ATZ2 composites will be attributed to its low grain size (0.37 ± 0.1 μm) compared to grain size in the ZTA2 composite (0.42 ± 0.1) μm. The measured grain size of zirconia in the ATZ2 composite and Al_2O_3 in the ZTA2 ones were 0.34 ± 0.06 and 0.42 ± 0.1, respectively, suggesting that the size of matrix grains dominates the compressive strength of the composites. It is well known that in compression the cracks do not behave like stress amplifiers and as result, the ceramic can handle compressive stresses

very well. Conversely, when the ceramic is placed in tension these cracks act as stress amplifiers where the dominant crack will quickly cut through the material, ending its life prematurely [59]. The Weibull plot ln ln [1/(1−*P*)] and ln H_v for ATZ2 (Fig. 6b) showed a poor fit suggesting that the changes observed in the slope for the seven intermediate and lowest three points indicate probably the presence of pores and microcracks with various orientations as well as a large range of flaw sizes that affect the Vickers hardness and consequently more than one mode of failure had occurred in the composites [60,61]. In fact, the ATZ2 is the composite with the lower Vickers hardness and sintered density (Fig. 2 and Table 4).

In spite of the low Weibull modulus for the tested materials, it is important to stress that there is a great possibility that the material with the highest Weibull Modulus in compressive strength and fracture toughness (ATZ2 nanocomposite) and Vickers hardness (ZTA2 nanocomposite), could be selected in a near future to be clinically tested and their efficiency to be demonstrated [62]. However, McCabe and Carrick [63] pointed out that 10 specimens were not enough to obtain reliable conclusions. We believe therefore that as the results for the above mentioned composites followed the Weibull curve, these have some useful validity, as for example, in applications where the loads during normal mastication ranging from 50 to 250 MPa, and 500–800 MPa in the case of parafunctional behavior such as bruxism [7,44,45]. These last requirements could be fulfilled with the compositions corresponding to ATZ system.

5. Conclusions

From the investigated ATZ and ZTA composites reinforced with Al_2O_3 whiskers, we can conclude the following:

1. Relative densities ranging from 93 to 98% were attained in the different composites at the processing temperature of 1500 °C for 2 h.
2. The composite with the highest characteristic strength and fracture toughness was the ATZ2 one. A wide range of compressive strength, fracture toughness, and Vickers hardness were obtained for all tested composites.
3. The addition of a low amount of Al_2O_3 whiskers seems to be enough to increase the hardness in the ZTA system. On the other hand, 2 wt.% Al_2O_3 whiskers are required to get high fracture toughness in ATZ composites.
4. The high fracture toughness in the ATZ2 composite could be attributed to the fracture mode which may result in greater fracture energy which leads to increase the fracture toughness values. Crack deflection, bridging grains as well as a high aspect ratio of the Al_2O_3 whiskers seem to be contributing to increasing the mechanical properties.
5. Some of the tested composites followed the Weibull curve having useful validity in applications where the loads during normal mastication and parafunctional behavior such as bruxism are high ranging from 50 to 1000 MPa in some cases depending on the location in the dentition.
6. Most important and reliable compressive strength test methods for materials which will be used in dental applications are needed prior to giving design recommendations.

Acknowledgements

The authors wish to express their appreciation to Wilber Antúnez and Karla Campos for invaluable SEM work. One of the authors (A. Nevárez-Rascón) thank the Consejo Nacional de Ciencia y Tecnología (CONACyT) for the financial support provided for this research work.

References

[1] Giordano R. A comparison of all-ceramic restorative systems, Part I. Gen dent 1999;47(6):566–70.
[2] van Dijken JW, Hasserlot L, Ormin A, Olofsson AL. Restorations with extensive dentin/enamel bonded coverage. A 5-year follow-up. Eur j oral sci 2001;109(4):222–9.
[3] Sadighpour L, Geramipanah F, Raeesi B. In vitro mechanical test for modern dental ceramics. J dent thran univ med sci 2006;3(3):143–52.
[4] Correa de Sá e Benevides de Moraes MC, Benavides de Moraes S, Nelson Elias C, Filho J, Guimarães de Oliveira L. Mechanical properties of alumina–zirconia composites for ceramic abutments. Mat res 2004;7(4):643–9.
[5] Studart AR, Filser F, Kocher P, Lüthy H, Gauckler LJ. Mechanical and fracture behavior of veneer-framework composites for all-ceramic dental bridges. Dent mater 2007;23:115–23.
[6] Lawn BR, Pajares A, Zhang Y, et al. Materials design in the performance of all-ceramic crowns. Biomaterials 2004;25:2885–92.
[7] Lüthy H, Filser F, Loeffel O, et al. Strength and reliability of four-unit all-ceramic posterior britges. Dent mater 2005;21:930–7.
[8] Anusavice KJ. Development and testing of ceramic for dental applications. Ceram trans 1995;48:101–24.
[9] Studart AR, Kocher P, Filser F, Gauckler LJ. Fatigue of zirconia under cyclic loading in water and its implications for the design of dental bridges. Dent mater 2006;23:106–14.
[10] Heimke G, Leyen S, Willmann G. Knee arthroplasty: recently developed ceramics offer new solutions. Biomaterials 2002;23:1539–51.
[11] Nikolay D, Kollenberg W, Deller K, Oswald M, Tontrup C. Manufacturing and properties of ZTA ceramics with nanoscaled ZrO_2. Proc eng 2006;4:E35–7.
[12] Leutbecher T, Hulsenberg D. Oxide fiber reinforced glass: a challenge to new composites. Adv eng mater 2000;3:93–9.
[13] Zhang X, Xu L, Du S, et al. Fabrication and mechanical properties of ZrB_2–SiCw ceramic matrix composite. Mater lett 2008;62:1058–60.
[14] Zhang X, Xu L, Du S, Han W, Han J. Crack-healing behavior of zirconium diboride composite reinforced with silicon carbide whiskers. Scr mater 2008;59:1222–5.
[15] Zhang X, Xu L, Han W, et al. Mirostructure and properties of silicon carbide whisker reinforced diboride ultra-high temperature ceramics. Solid state sci 2009;11:156–61.
[16] Xu HHK, Martin TA, Antonucci JM, Eichmiller FC. Ceramic whisker reinforcement of dental resin composites. J dent res 1999;78:706–12.
[17] Evans AG. High toughness ceramics. Mater sci eng 1998;A105/106:65–75.
[18] Becher PF. Toughening behavior in ceramics associated with the deformation of tetragonal zirconia. Acta metall 1986;34:1885–91.
[19] Hsueh CH. Some considerations of evaluation of interfacial frictional stress from the indentation technique for fibre-reinforced ceramic composites. J mater sci lett 1989;8:739–42.
[20] De Aza AH, Chevalier J, Fantozzi G. Crack growth resistance of alumina, zirconia and zirconia toughened alumina ceramics for joint prostheses. Biomaterials 2002;23:937–45.
[21] Ruhle M, Stecker A, Waidelich D, Kraus B. In situ observations of stress-induced phase transformation in ZrO_2 containing ceramics. In: Claussen N, Rulle M, Heuer A, editors. Advanced in Ceramics. Science and Technology II. Columbus: American Ceramic Society; 1984.
[22] Gregori G, Burger W, Sergo V. Piezo-spectroscopic analysis of the residual stress in zirconia-toughened alumina ceramics: the influence of the tetragonal-to-monoclinic transformation. Mater sci eng 1999:401–6.
[23] Guazzato M, Albakry M, Ringer SP, Swain MV. Strength, fracture toughness and microstructure of a selection of all-ceramic materials. Part II. Zirconia-based dental ceramics. Dent mater 2004;20:449–56.
[24] Rizcalla AS, Jones DW. Mechanical properties of commercial high strength ceramic core materials. Dent mater 2004;20:207–12.
[25] Yang SF, Yang LQ, Jin ZH, et al. New nano-sized Al_2O_3–BN coating 3Y-TZP ceramic composite for CAD/CAM-produced all-ceramic dental restorations Part I. Fabrication of powders. Nanomed nanotechnol 2009;5:232–9.
[26] Garvie RC, Hannink RHJ, Pascoe RT. Ceramic steel? Nature 1975;258:703–4.
[27] Quinn JB, Quinn GD. A practical and systematic review of Weibull statistics for reporting strengths of dental materials. Dent mater 2010;26:135–47.
[28] Fett T, Ernst E, Munz D, Badenheim D, Oberacker R. Weibull analysis of ceramics under high stress gradients. J eur ceram soc 2003;23:2031–7.
[29] Zhao YY, Ma E, Xu J. Reliability and compressive fracture strength of Mg–Zn–Ca bula metallic glasses: flaw sensivity and Weibull statistics. Scr mater 2008;58:496–9.
[30] Danzer R, Supancic P, Pascual J, Lube T. Fracture statistics of ceramics — Weibull statistics and deviations from Weibull statistics. Eng fract mech 2007;74:2919–32.
[31] Weibull WA. A statistical theory of strength of materials. R Swed Inst Eng Res 1939:1–45.
[32] Weibull WA. *A statistical distribution function of wide applicability*. 1951;18:293–97.
[33] Khalili KK. Statistical properties of Weibull stimators. J mater sci 1991;26:6741–52.
[34] Saghafi A, Mirhabibi AR, Yari GH. Improved linear regression method for estimating Weibull parameters. Theor appl fract mech 2009;52:180–2.
[35] Guazzato M, Albakry M, Swain MV, Ironside J. Mechanical properties of In-Ceram alumina and In-Ceram zirconia. Int j prosthodont 2002;15(4):339–46.
[36] Tinschert J, Zwaz D, Marx R, Anusavice KJ. Structural reliability of alumina-, feldspar-, leucite-, mica-, and zirconia-based ceramics. J dent 2000;28(7):529–35.
[37] Bona AD, Anusavice KJ, DeHoff PH. Weibull analysis and flexural strength of hot-pressed core and veneered ceramic structures. Dent mater 2003;19(7):662–9.

[38] Papargyris AD. Estimator type and population size for estimating the Weibull modulus in ceramics. J eur ceram soc 1998;18:451–5.
[39] Jayatilaka ADeS. Fracture of engineering brittle materials. Appl sci lond 1979.
[40] Trustrum K, Jayatilaka ADeS. On estimating the Weibull modulus for a brittle material. J mater sci 1979;14:1080–4.
[41] Bergman B. On the estimation of the Weibull modulus. J mater sci 1984;3:689–92.
[42] Green NR, Campbell J. Statistical distributions of fracture strengths of cast Al–7Si–Mg Alloy. Mater sci eng 1993;173A:261–6.
[43] Gong J, Chen Y, Li C. Statistical analysis of fracture toughness of soda-lime glass determined by indentation. J noncryst solids 2001;279:219–23.
[44] Kelly JR. Clinical failure of dental ceramic structures: insights from combined fractography, in vitro testing and finite element analysis. Ceram trans 1995;48: 125–37.
[45] Kelly JR. Ceramics in restorative and prosthetic dentistry. Ann rev mater sci 1997;27:443–68.
[46] ASTM C 1424-99, *Standard Test Method for Compressive Strength of Advanced Ceramics at Ambient Temperature ics*, 1999.
[47] ASTM C 1327-99, *Standard Test Method for Vickers indentation hardness of advanced ceramics*, 1999.
[48] Evans AG, Charles EA. Fracture toughness determinations by indentation. J Am Ceram Soc 1976;59:371–2.
[49] Cho Y-K, Kim B-M, Yoon S-Y, Stevens R, Park H-C. A novel processing route for whisker shaped mullite–alumina composites from kaolin. J ceram proc res 2008;9:652–6.
[50] Tekeli S. Fracture toughness (KIC), hardness, sintering and grain growth behaviour of YSCZ/Al2O3 composites produced by colloidal processing. J alloy compd 2005;391:217–24.
[51] Bengisu M, Inal OT. Whisker toughening of ceramics: toughening mechanisms, fabrication and composite properties. Annu rev mater sci 1994;24:83–124.
[52] Chakravarty D, Bysakh S, Muraleedhran K, Narasigna Rao T, Sundaresan R. Spark plasma sintering of magnesia-doped alumina with high hardness and fracture toughness. J Am Ceram Soc 2008;91:203–8.
[53] Nevarez-Rascon A, Aguilar-Elguezabal A, Orrantia E, Bocanegra-Bernal MH. Al2O3 (w)–Al2O3(n)–ZrO2 (TZ-3Y)n multi-scale nanocomposite: an alternative for different dental applications? Acta biomater 2010;6:563–70.
[54] Sneary PR, Yeh Z, Crimp MJ. Effect of whisker aspect ratio on the density and fracture toughness of SiC whisker-reinforced Si3N4. J mater sci 2001;36: 2529–34.
[55] Becher PF, Hsueh CH, Angelini P, Tiegs TN. 1061 Toughening behavior of whisker-reinforced ceramic matrix composites. J Am Ceram Soc 1988;71:1050–61.
[56] Lipson C, Sheth NJ. Statistical distributions. Statistical design and analysis of engineering experimentsNew York: McGraw Hill; 1973.
[57] Tiryakioglu M, Hudak D, Ökten G. On evaluation Weibull fits to mechanical testing data. Mater sci eng a 2009;527:397–9.
[58] Doremus RH. Fracture statistics: a comparison of the normal Weibull and type I extreme value distributions. J appl phys 1983;54:193–201.
[59] http://www.sv.vt.edu/classes/MSE2094_NoteBook/97ClassProj/exper/mcmurtry/www/matt.html, accessed on May 03 2010-05-20.
[60] Stewardson DA, Shortall AC, Marquis PM, Lumley PJ. The flexural properties of endodontic post materials. Dent mater 2010, doi:10.1016/j.dental.2010.03.017.
[61] Fleming GJP, Jandu HS, Nolan L, Shaini FJ. The influence of alumina abrasion and cement lute on the strength of a porcelain laminate veneering material. J dent 2004;32(1):67–74.
[62] Burrow MF, Thomas D, Swain MV, Tyas MJ. Analysis of tensile bond strengths using Weibull statistics. Biomaterials 2004;25:5031–5.
[63] McCabe JF, Carrick TE. A statistical approach to the mechanical testing of dental materials. Dent mater 1986;2:139–42.